JOURNAL OF MATERIALS SCIENCE **36** (2001) 5757–5765

Cyclic stress response and fatigue behavior of Cu added ferritic steels

T. YOKOI*, M. TAKAHASHI
Steel Products Lab.-1, Steel Research Laboratories, Technical Development Bureau, Nippon Steel Corporation, 20-1, Shintomi, Futtsu, Chiba, 293-8511, Japan
E-mail: t-yokoi@oita.nsc.co.jp

N. MARUYAMA, M. SUGIYAMA
Materials Characterization Research Lab., Advanced Technology Research Laboratories, Technical Development Bureau, Nippon Steel Corporation 20-1, Shintomi, Futtsu, Chiba, 293-8511, Japan

Steels in which Cu content was altered from 0 to 1.5 mass% were subjected to various heat treatments to change the state of Cu. Concerning these respective steels, fatigue ratio by a stress controlled fatigue test and fatigue resistance by a strain controlled fatigue test thereof were compared. Furthermore dislocation substructure and surface defect during and after cyclic straining were investigated to clarify the effect of Cu on fatigue properties. The fatigue ratios at 2.0×10^6 loading cycles of the Cu added steels after aged at 450 and 750 degrees C are 0.7, remarkably high as compared with those of the Cu added steels after aged at 550 and 650 degrees C, the Cu free steels and any other conventional steels whose fatigue ratio are approximately between 0.5 and 0.6. The fatigue resistance of the as-rolled Cu added steel maintains steady cyclic hardening until fracture. To the contrary the Cu added steel after heat treatment at 550 degrees C shows cyclic hardening to the peak stress and then shows a cyclic softening until fracture. The surface roughness of the Cu added steels after cyclic straining are relatively shallow compared with those of the Cu free steel. The internal substructure of the Cu free steel shows typical cell structure but those of the Cu added steels exhibit vein structure.

1. Introduction

The solubility of Cu in ferrite at room temperature is very small so that ferrite can hardly contain Cu in solution at room temperature in equilibrium. But the solubility of Cu above 800 degrees C is about 2 mass% and the ferrite matrix can be supersaturated with Cu by rapidly cooling from high temperatures to room temperature. Subsequent aging can precipitate Cu in ferrite. In early stage of Cu precipitation in the ferrite matrix during aging, coherent b.c.c. Cu-rich clusters nucleate and grow in the supersaturated ferrite matrix. Further Cu-rich clusters change to coherent b.c.c. Cu precipitates. The process can be described in terms of the formation and growth of coherent b.c.c. Cu precipitates and the consequent transformation of them into incoherent f.c.c. Cu particles [1, 2].

It is well known that Cu in steels increases the strength thereof remarkably due to Cu precipitation. It is also reported that Cu precipitation has a beneficial effect on fatigue strength. For example, McGrath and Bratina [3] reported that, while a 1.5 mass% Cu alloy hardened by Cu precipitates was subjected to fatigue, a state of reversion was not reached during which the Cu particles would dissolve in the ferrite matrix. In addition to this, Le May [4] reported that slight overaging beyond peak tensile strength to produce a fine dispersion of incoherent Cu particles in steels has a beneficial effect on fatigue properties. It has been suggested that the effectiveness of Cu precipitates in improving fatigue strength depends on their state. Large incoherent Cu precipitates are more effective in restricting dislocation movement under cyclic straining than fine Cu precipitates and clusters. Fournelle *et al.* [5] reported that quenched and tempered medium carbon steels containing fine coherent precipitates of Cu exhibited high resistance to fatigue crack initiation in notched specimens as well as displaying high cyclic fatigue resistance, and they suggested that this improvement is due to the stabilizing effect of fine coherent precipitates on the dislocation substructure. But the mechanisms causing Cu to have this effect on fatigue behavior have not yet been clarified in details.

In this investigation, the stress controlled fatigue strengths and strain controlled fatigue resistance of the Cu free and Cu added steels under different precipitation conditions have been compared in terms of dislocation substructures and surface roughness during and after cyclic loading. The purpose of this paper is to

Present address: Oita R&D Lab., Technical Development Bureau, Nippon Steel Corporation 1, Oaza Nishinosu, Oita-city, Oita, 870-0992, Japan.

clarify the cause that Cu addition to steels is effective in fatigue strength and Cu precipitates in steels are less beneficial to fatigue strength than to tensile strength.

2. Experimental procedure

2.1. Materials and heat treatment

The chemical composition of steels used in this study is shown in Table I. The amount of Cu was altered from 0 to 1.5 mass% in titanium stabilized ultra low carbon steels. The steels were melted in a 300 kg vacuum furnace and then cast into 100 kg ingots respectively. Fig. 1 shows the process of making hot bands. Those ingots reheated to 1200 degrees C were previously hot-rolled to have a thickness of 40 mm. The 40 mm-thick hot bands were soaked for 0.5 hour at 1050 degrees C, hot-rolled to have a thickness of 5 mm and cooled by 40 degrees C/s to room temperature. The hot rolling finishing temperature (FT) of the hot bands was above their Ar3 temperature. Fig. 2 shows the optical micrographs at 1/4 thickness of the hot bands before heat treatment. Regardless of Cu content, ferrite grain sizes of the hot bands are almost the same.

TABLE I Chemical compositions of investigated steels

Steel	C	Si	Mn	P	S	Al	Ti	N	Cu
A	0.0018	0.01	0.20	0.004	0.004	0.04	0.05	0.0016	<0.002
B	0.0020	0.01	0.20	0.004	0.004	0.04	0.05	0.0016	1.51

Values in mass%.

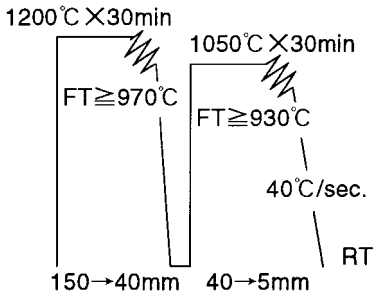

Figure 1 Process of hot rolling.

TABLE II Heat treatment and expected Cu state of specimens

Specimen	Heat treatment	Cu state
A	As rolled	Cu free
B1	As rolled	Solid solution
B2	550° × 60 min	Fine precipitation

After hot rolling, some of the hot bands were subjected to heat treatments to change the state of Cu in ferrite by changing the aging temperature between 450 and 750 degrees C at 100 degrees C intervals for 1 hour and followed by air cooling to room temperature. Other hot bands were as-rolled in order to keep the Cu in a solid solution. Heat treatments and expected Cu states of the specimens are shown in Table II.

2.2. Tensile test

Tensile tests were performed using the JIS 5 type specimen. All of the tensile specimens were cut with their long axis lying in the rolling direction of the hot bands.

2.3. Stress controlled fatigue test

Stress controlled fatigue test specimens were used as shown in Fig. 3. The specimens were cut with their

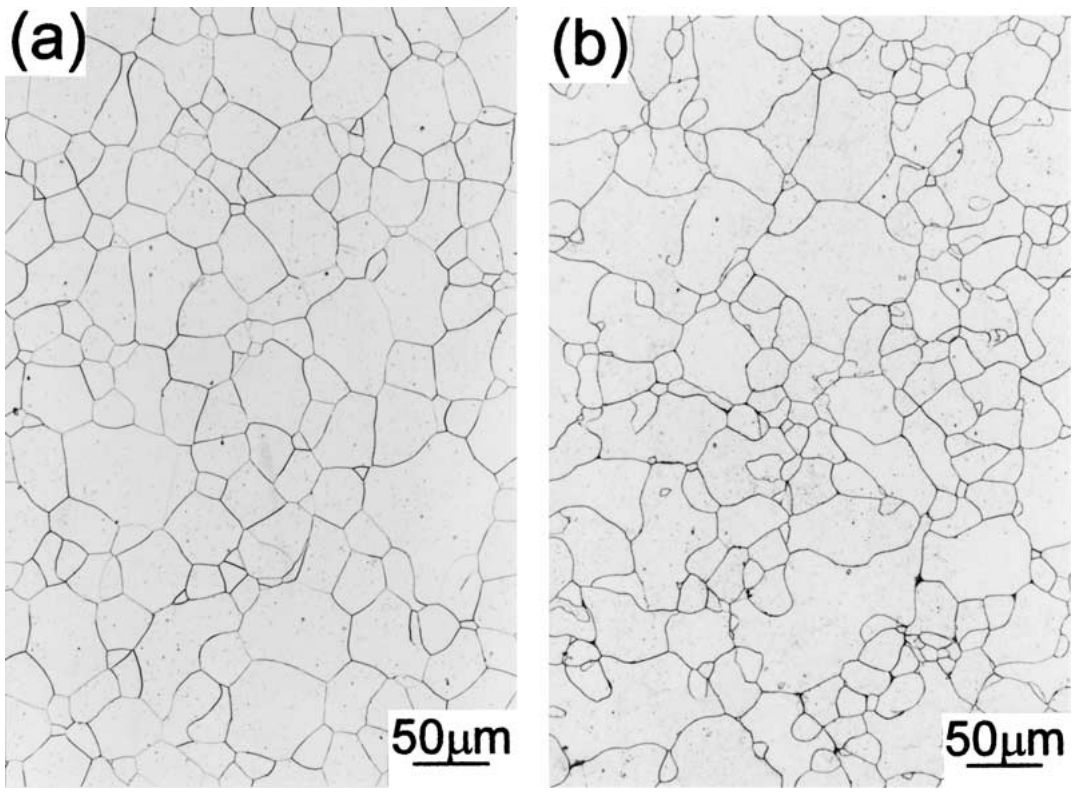

Figure 2 Optical micrographs of microstructure of investigated steels. (a) Steel A (Cu free), (b) steel B (Cu added).

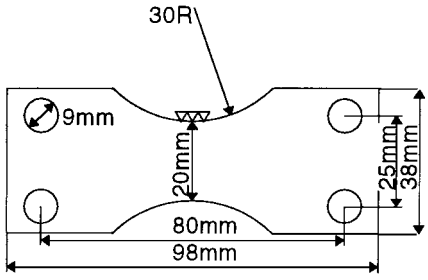

Figure 3 Dimension of the specimen for stress controlled fatigue test (plane bending test).

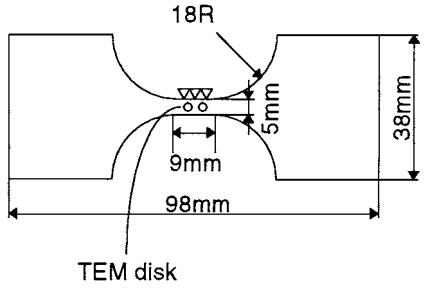

Figure 4 Dimension of the specimen for strain controlled fatigue test (axial tension-compression test).

long axis lying along the rolling direction of the hot bands and ground on both faces to avoid any influence of the surface. The stress controlled fatigue test was performed by plane bending with a SHIMAZU closed-loop electrohydraulic servo controlled testing machine with 50 kN of the maximum load under an R ratio of -1 at a frequency between 5 and 15 Hz and with a sine wave form.

2.4. Strain controlled fatigue test

A strain controlled fatigue test specimen is illustrated in Fig. 4. The specimens were prepared in accordance with the same procedure as that used to prepare the stress controlled fatigue test specimens. Some of these strain controlled fatigue test specimens were chemically polished to be able to observe the surface roughness due to cyclic straining. The strain controlled fatigue test was conducted by axial tension-compression with an MTS closed-loop electrohydraulic servo controlled testing machine of 100 kN capacity and the specimens were tested with a strain ratio R of -1 at a strain rate of 4×10^{-3}/sec and with a triangular wave form.

2.5. Surface roughness

The surface roughness of the specimens during the fatigue test was observed under a scanning laser microscope of the LASERTEC 1LM11 type.

2.6. Electron Microscopy

In order to investigate the effects of Cu in ferrite on a microstructure, thin foils for a transmission electron microscope were prepared from the middle of the gage section of the strain controlled fatigue test specimens in 1/4 thickness as shown in Fig. 4. The foils were studied under a 400 kV transmission electron microscope (TEM) of the JEOL 4000FX type and a 200 kV TEM of the HITACHI HF2000 type with a field emission gun. Energy dispersive X-ray spectroscopy was also applied to analyze Cu content in ferrite.

3. Experimental results

3.1. Effect of the state of Cu on fatigue strength

Fig. 5 shows the results of the tensile tests. Tensile properties are plotted vs. the aging temperature. The tensile strength increases as Cu content increases at the same heat treatment temperature. The tensile strength of the Cu free steels was fairly independent of the aging temperature. However, remarkable increases in the tensile strength of the Cu added steel can be observed after the heat treatment at 550 and 650 degrees C. This may be due to fine Cu precipitates.

Fig. 6 shows the fatigue strength plotted vs. the heat treatment temperature. In this paper, the term "fatigue strength" is defined as the highest stress amplitude at which fracture does not occur even after 2.0×10^6 loading cycles. The fatigue strength increases as Cu content increases at the same heat treatment temperature. But a remarkable increase in the fatigue strength is not

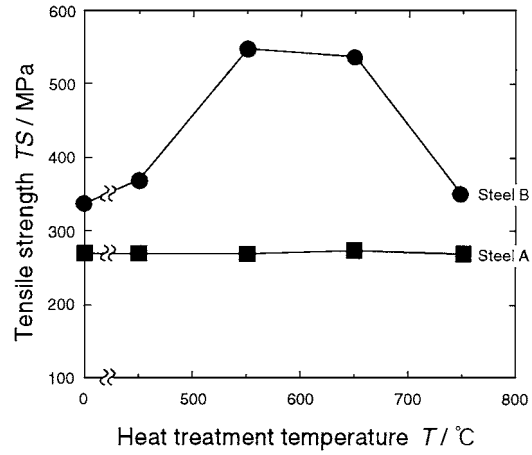

Figure 5 Effect of heat treatment temperature on tensile strengths of the two investigated steels.

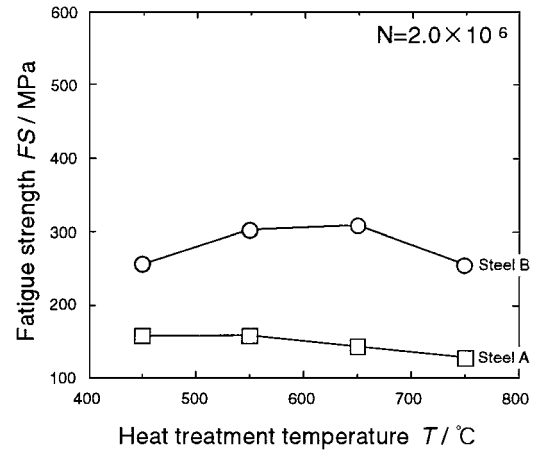

Figure 6 Effect of heat treatment temperature on fatigue strengths at 2.0×10^6 of the two investigated steels.

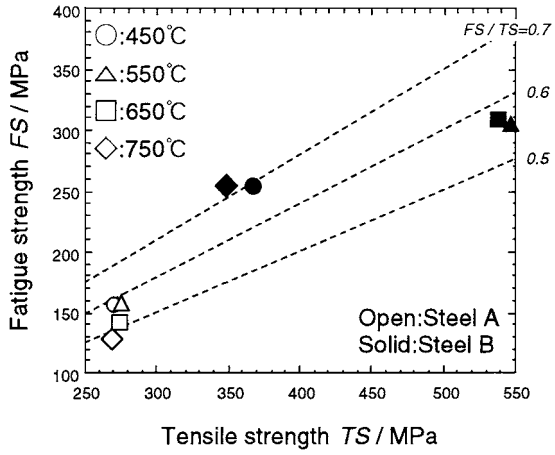

Figure 7 Relationship between tensile strength and fatigue strength of investigated specimens.

obtained for all the Cu added steels. This result indicates that the effect of fine Cu precipitation hardening on fatigue strength is less effective than that on tensile strength.

The fatigue strength is plotted vs. the tensile strength as shown in Fig. 7. In this paper, the fatigue ratio means the fatigue strength normalized by the tensile strength. The fatigue ratio of the Cu added steels after aged at 450 and 750 degrees C is superior to that of the Cu free steel. But the fatigue ratio of the Cu added steels after aged at 550 or 650 degrees C is almost the same as that of the Cu free steels. The fatigue ratio of 0.7 of the Cu added steel at 450 and 750 degrees C is remarkably high as compared with the fatigue ratio between 0.5 and 0.6 for conventional steels. The Cu added steel at 450 degrees C is hardened by the Cu in solid solution or Cu clusters and the Cu added steel at 750 degrees C contains coarse Cu particles and Cu in solid solution. This result indicates that the effect of the solid solution hardening of Cu on fatigue strength is greater than that of the fine precipitation hardening. It seems that the Cu in solid solution or cluster has a great effect on fatigue strength. It is therefore concluded that Cu in solid solution or Cu clusters is more likely than fine Cu precipitates to increase the fatigue strength of ferritic steels.

It is well established that the fatigue process can be roughly divided into four stages: cyclic hardening/softening, crack initiation, crack propagation and fracture. In flaw-free materials, a significant fraction of the total life passes before crack initiation. Namely, it is important to increase the resistance against the initiate of cracks in order to improve fatigue strength or fatigue life. Therefore, the cyclic deformation behavior of these steels was investigated.

3.2. Cyclic deformation behavior

To clarify the effect of Cu addition and the state of Cu on fatigue behavior, two specimens, which were as-rolled and heat treated at 550 degrees C, were studied. Fig. 8 is the stress response curve and shows the results of the strain controlled fatigue tests. All of the tests were performed at 0.3% of total strain amplitude. In the Cu free steel, there was no difference in the shape of the

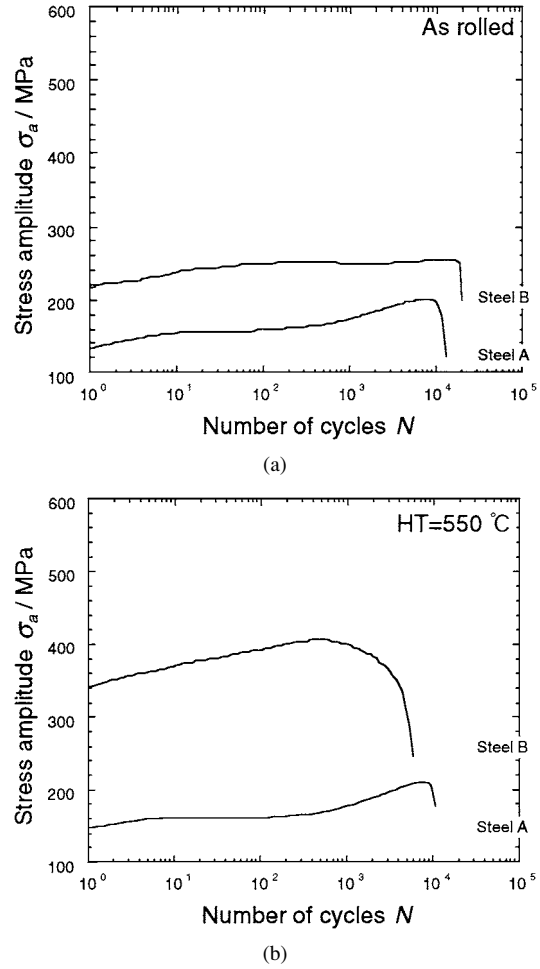

Figure 8 Cyclic stress response curves at total strain amplitude, 0.3%. (a) As-rolled, (b) 550°C × 60 min.

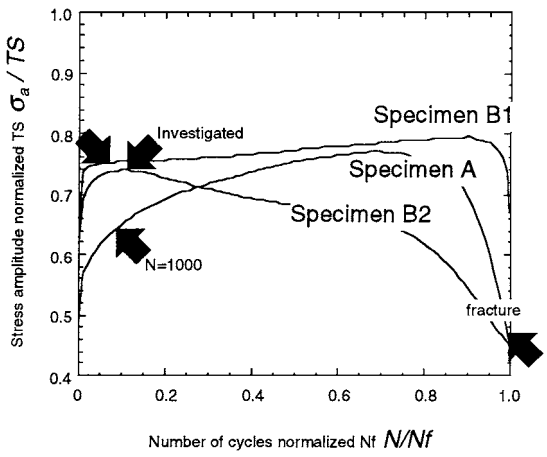

Figure 9 Cyclic stress response behaviors for the three investigated specimens.

stress response curve between before and after aging at 550 degrees C, but in the Cu added steel, the difference in the shape of the stress response curves can be seen.

In order to exam the roll of Cu during cyclic straining, the stress response curves normalized by the tensile strength were plotted vs. the number of cycles N normalized by the number of fracture cycles Nf in Fig. 9. The as-rolled Cu added steel, B1, shows steady cyclic hardening until the late stage of the fatigue life. The Cu added steel after heat treatment at 550 degrees C, B2,

shows, in contrast, cyclic hardening to the peak stress amplitude at the early stage of the fatigue life and then shows cyclic softening until fracture.

3.3. Surface

The surface roughness of the specimens after fatigue tests was observed with the scanning laser microscope. It is well established that a surface roughness is considered to be an initiation site of fatigue cracks and then the surface roughness will grow into intrusions and extrusions. Fig. 10 shows the distribution of step depths of roughness caused by the slips in ferrite grains after 1000 cycles. The slip steps in the Cu added steels are relatively shallow compared with those in the Cu free steel. This is due to the effect of Cu addition on the steels. The shallow slip steps on the surface can prevent an increase in stress concentration factor on the surface, and result in longer crack initiation time.

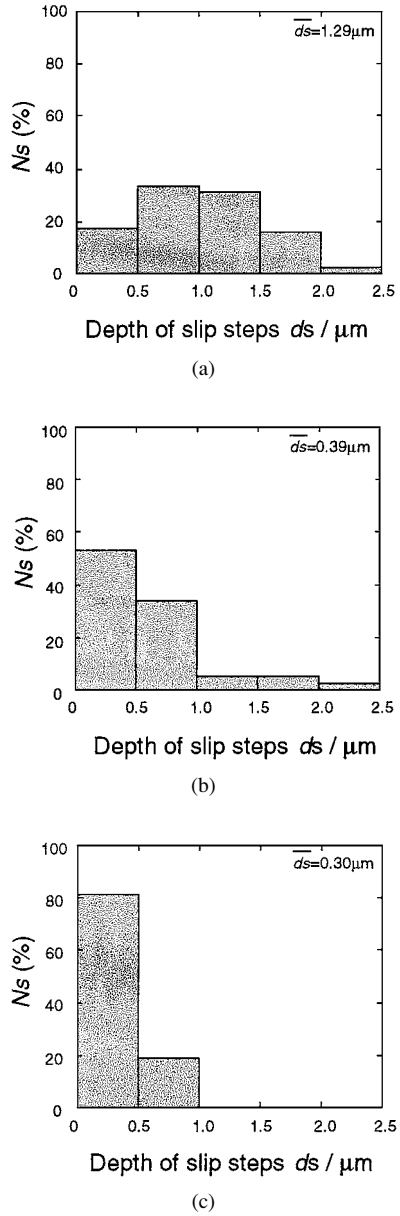

Figure 10 Distribution histograms of depth for slip steps on the surface of specimens. (a) Specimen A (Cu free), (b) specimen B1 (Cu solid solution), (c) specimen B2 (Cu precipitation).

3.4. TEM micrograph

Fig. 11 shows the TEM micrograph of specimens after 1000 cycles of the fatigue test. 1000 cycles correspond to about 1/10 of Nf as shown in Fig. 9. At those cycles, specimen B2 still shows cyclic hardening before the peak stress.

Specimen A already indicates a typical cell structure. On the other hand, Specimen B1 still shows a vein structure and specimen B2 still shows a "planar array" dislocation arrangement.

A TEM micrograph of specimens after rupture is shown in Fig. 12. Specimen A still shows the cell structure. Specimens B1 and B2 show the vein structure, respectively.

The substructures of specimen A and B1 do not show significant changes even after the rupture. In particular, the result of specimen B1 corresponds to the steady state of the stress response in Fig. 9. Although the specimen B2 shows the planar array dislocation arrangement at 1000 cycles, the dislocation structure changes to the vein structure after the rupture. The substructure of the specimen B2 obviously resembles that of the specimen B1. These observations suggest that Cu precipitates retard the formation of the vein structure only at the early stage of fatigue life, however their effect on fatigue strength at the late stage of fatigue life is lost.

4. Discussion

The experimental results and observations are summarized in Table III. The fatigue ratio (FS/TS) of the Cu solid solution steel is superior to that of Cu free steel. The reason for why Cu in solid solution increases fatigue ratio has a connection with that the Cu solid solution hardened steel shows steady cyclic hardening from the early stage of the fatigue life to fracture, while the Cu free steel shows slightly gradual cyclic hardening. Namely, the Cu solid solution hardened steel has high resistance against cyclic deformation caused by dislocation motion and thus the fatigue crack initiation due to slips is retarded. In practice, the observation of the surface shows that the slip steps of the Cu added steels are finer than those of Cu free steel, as shown in Fig. 10.

Feltner and Laird reported that the saturated substructures in the bulk of f.c.c. metals, of which specimens were tested by a strain controlled fatigue test, are determined only by the amplitude of cycling and the stacking-fault energy [6–8]. In the case of other metals, b.c.c. metals, for which stacking-fault energy cannot be determined, cross-slip frequency can be used instead of stacking-fault energy [9–11].

Regarding the cross-slip frequency, the following reports have been recognized. An easy cross-slip metal, e.g. pure iron, under high amplitude loading exhibits a cell structure [12]. A difficult cross-slip metal, e.g. Fe–Si alloy, under low amplitude loading shows a planar-array dislocation arrangement because the dislocations can not leave their primary slip plane. A substructure of a difficult cross-slip metal under high amplitude loading consists of veins, irregular bands or patches of line dislocations, dislocation loops and debris [13].

TABLE III Stress controlled fatigue properties and strain controlled fatigue behaviors including substructures and surface condition

Specimen	FS/TS	Cyclic response	Substructure		Slip steps
			$N = 1000$	Rupture	$N = 1000$
A	0.58	Gradually hardening	Cell-structure	Cell-structure	Deep
B1	0.69	Steady hardening	Vein-structure	Vein-structure	Shallow
B2	0.55	Softening from peak	Planar-array	Vein-structure	Shallow

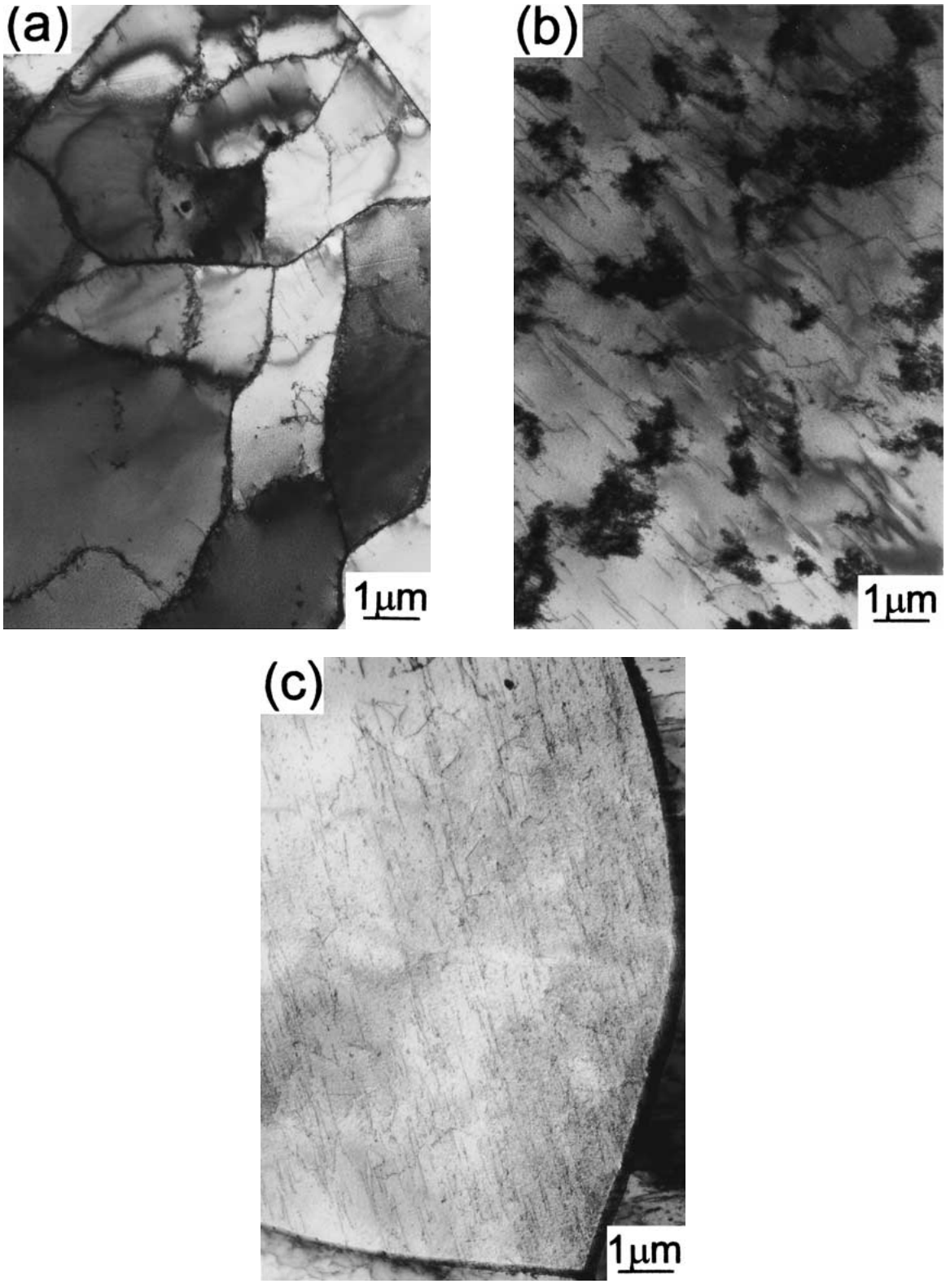

Figure 11 TEM micrographs of specimens at 1/10Nf cycles. (a) Specimen A (Cu free), (b) specimen B1 (Cu solid solution), (c) specimen B2 (Cu precipitation).

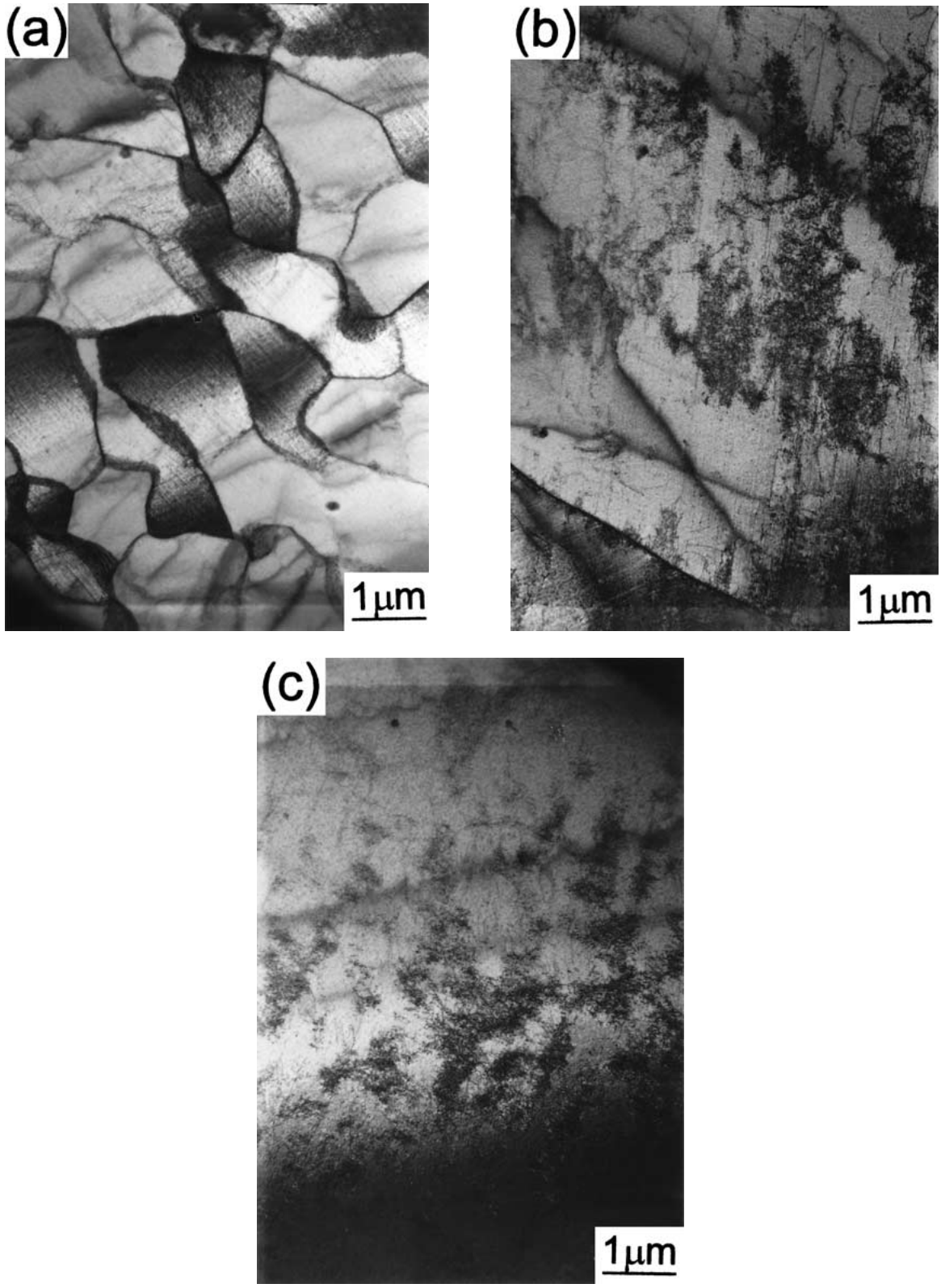

Figure 12 TEM micrographs of ruptured specimens. (a) Specimen A (Cu free), (b) specimen B1 (Cu solid solution), (c) specimen B2 (Cu precipitation).

On the other hand, it is well established that plastic strain is necessary for inducement of fatigue fracture in metals. Not only cross-slip frequency but also cumulative plastic strain influences the formation of dislocation structure.

In the present work, the addition of Cu to the steels changes the substructure of the steels from a cell structure to a vein structure or a planar-array dislocation arrangement at the early stage. Additional cycles to fracture change the planar-array dislocation arrangement into the vein structure in the Cu precipitation hardened steel as shown in Table III.

These results suggest that the addition of Cu to the steels reduce the cross-slip frequency of the steels and consequently change the dislocation structure during cyclic loading. Cyclic softening of the Cu precipitation hardened steel in total strain controlled test induces the plastic strain, so the planar-array dislocation

arrangement develops the vein structure at the late stage of the fatigue.

Furthermore, according to previous work, the substructure in the surface layer on a variety of metals and alloys was also studied. The results of all these investigations show that the dislocation structures in the surface layer depend on the cross-slip frequency and on the amplitude in the same way as the bulk [14]. The formation of the surface intrusions and extrusions is deeply related to PSBs (Persistent Slip Bands) and the formation of the PSBs, which is not formed in difficult cross-slip metals, requires the cross-slip. In the case of easy cross-slip metals, the marked surface defect can be seen. The surface extrusions and intrusions can be described as valleys and hills lying mainly along the intersection lines of the slip plane with the surface of the specimen. Formation of the coarse slip must be related to the collective motion of dislocations within the whole layers of cells lying along the slip plane. The basic mechanism lies again in bowing-out dislocation segments from cell walls, their reaching the nearest wall and thus causing an avalanche along the whole layer of cells [15]. Concerning difficult cross-slip metals, the surface defect looks regularly saw-like to some extent and resembles a card slip. The fine slip, which subsequently gives way to the formation of coarse slips in metals with easier cross slips, continues to operate. The fine slip mechanism continues to the end of fatigue life [16].

As mentioned above, the addition of Cu to the steels refines surface roughness. Fig. 13 is a schematic diagram of the fatigued surface on the Cu added steel and the Cu free steel respectively. The Cu added steel has fine slip steps but the Cu free steel has coarse slip steps. Therefore the fine slip steps have a smaller amount of stress concentration than that of the coarse slip steps and the addition of Cu consequently retards fatigue crack nucleation.

On the other hand, the fatigue ratio of the Cu precipitation hardened steel is inferior to that of Cu solid solution steel. The reason for this inferior fatigue ratio is that the Cu precipitation hardened steel shows cyclic hardening to the peak stress amplitude at the early stage of the fatigue life and then shows cyclic softening until fracture. Namely, cyclic straining loses the effect of precipitation hardening on fatigue strength.

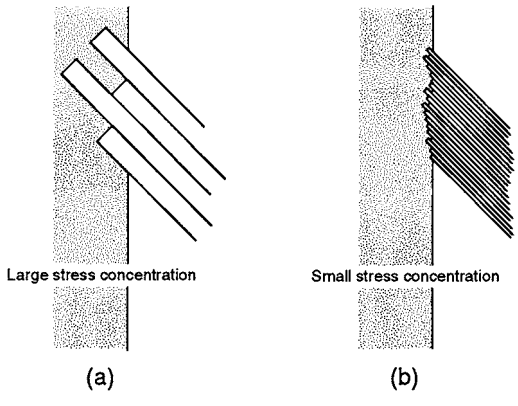

Figure 13 Schematic illustrations of slip steps growing into intrusions and extrusions on the surface. (a) Easy cross slips metals, (b) difficult cross slip metals.

TABLE IV Quantitative EDS analyses in Cu segregation

Specimen	On matrix	In dislocation
B1 (solid solution)	1.57 mass%	1.57 mass%
B2 (precipitation)	1.52 mass%	2.85 mass%

Precipitates and foreign particles retard the formation of a saturation dislocation structure [17]. The fine Cu precipitated steel before 1000 cycles corresponded to about 1/10 Nf exhibits planar array dislocation arrangements as shown in Fig. 11c, but after fracture the dislocation structure of this steel changes to the vein structure in Fig. 12c. These observations suggest that the fine coherent Cu precipitates in steel lose the inhibition against dislocation motion during cyclic loading, hence the cyclic softening and the change of the dislocation structure occur.

To understand the reason why cyclic straining loses the effect of the fine Cu precipitates on fatigue strength during the fatigue test, the Cu precipitates was directly observed. Fig. 14a and b are the TEM micrograph and the EDS spectrum of the specimen B2 after 1000 cycles of the fatigue test, respectively. The small circle in Fig. 14a indicates an example of a point of an EDS analysis. A peak spectrum of Cu element was detected at this point in a dislocation as shown in Fig. 14b. Needless to say, the peak spectrum of Cu element was detected not only at this point but also almost all the points in the dislocation. The EDS analysis is concluded in Table IV, which indicates that the Cu content in dislocations in the Cu solid solution steel is not different from that in matrix. But in the fine Cu precipitated steel, the amount of Cu content in dislocations is higher than in matrix. This result shows that Cu become denser and segregate into the dislocation in the Cu precipitated steel. In other words, it is likely that the repeated cutting of the precipitates by moving dislocations lead to dissolution of the precipitates. The dissolved Cu segregates on the dislocations in the Cu precipitated steel.

Fig. 15 illustrates the particle shearing mechanism. If a dislocation passes through a coherent or partly coherent particle, the particle is split into two parts, which are shifted along a slip plane. The repeated "to-and-fro" motion of dislocations in fatigue may reduce the average particle size to a point at which particles become thermodynamically unstable and revert to solid solution [18]. Moreover, it is reported that the Cu particles in Fe–Cu alloy can be cut by dislocations and the change in dislocation configuration in Fe–Cu alloy aged to maximum strength can be taken as evidence of Cu particle cutting [19, 20]. The mechanism of behavior under cyclic straining for the Cu precipitated steel can be summed up as follows; Cu precipitates can be obstacles to the dislocation motion at the early stage of the fatigue process. Remarkable cyclic hardening takes place. Consequently, the cyclic softening occurs from the peak stress to fracture. Because the Cu precipitates are cut by the moving dislocations and become too small to be stable, the dissolution of the precipitates takes place.

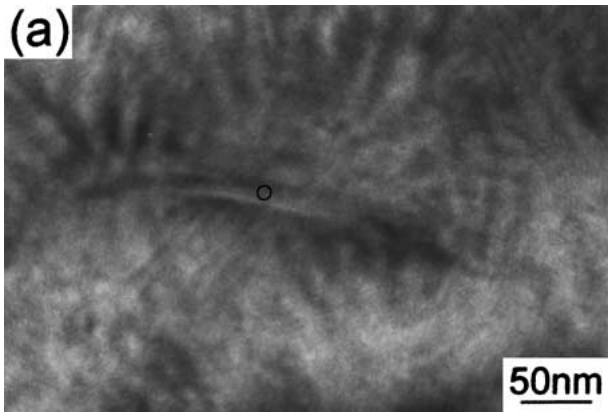

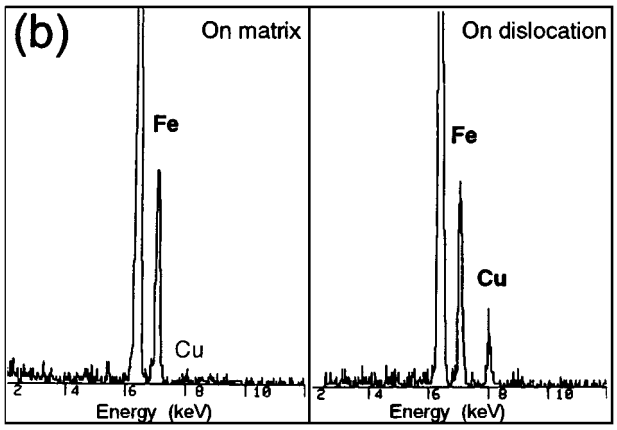

Figure 14 Results of the TEM observation and the EDS analysis. (a) TEM micrograph in a dislocation. Arrowhead indicates an analyzed point for the EDS. (b) EDS spectra on matrix and in a dislocation.

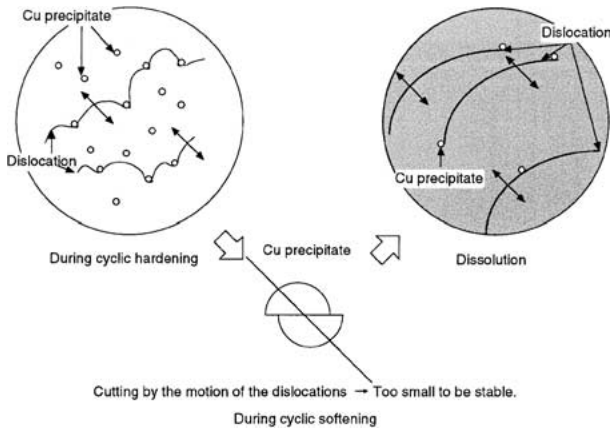

Figure 15 Schematic representation of dissolution process of Cu precipitates during cyclic softening.

5. Conclusion

The stress controlled fatigue limits and strain controlled fatigue strength of the Cu free and Cu added steels under different precipitation conditions have been compared in terms of dislocation substructures and surface roughness during and after cyclic loading in order to clarify the effect of Cu on fatigue properties. The results can be summarized as follows:

1. The solute Cu in ferrite has an effect on fatigue strength, because the solute Cu changes the dislocation substructure from the cell structure into the vein structure. Further the addition of Cu refines the slip steps at the surface.

2. The effect of the fine Cu precipitates in ferrite on fatigue strength is less than its effect on tensile strength. Although the fine Cu precipitates retard the formation of the vein structure in the early stage of the fatigue life, the repeated cutting of the precipitates by "to-and-fro motion" of dislocations lead to dissolution of precipitates and thus the effect of the fine Cu precipitates is lost.

Acknowledgements

One of the authors would like to thank to Mr. G. Shigesato for help with transmission electron microscopy and we are indebted to Dr. K. Kishida for his detailed criticism of this study.

References

1. G. M. WORRALL, J. T. BUSWELL, C. A. ENGLISH, M. G. HETHERINGTON and G. D. W. SMITH, *J. Nucl. Mater.* **148** (1987) 107.
2. P. J. OTHEN, M. L. JENKINS and G. D. W. SMITH, *Phil. Mag.* A **70** (1) (1994) 1.
3. J. T. MCGRATH and W. J. BRATINA, *Phil. Mag.* **21** (1970) 1087.
4. I. LE MAY, *J. Materials* **6** (1971) 436.
5. R. A. FOURNELLE, E. A. GREY and M. E. FINE, *Met. Trans.* A**7** (1976) 669.
6. C. E. FELTNER and C. LAIRD, *Acta Met.* **15** (1967) 1621.
7. *Idem.*, *ibid.* **15** (1967) 1633.
8. *Idem.*, *Trans. AIME* **242** (1968) 1253.
9. A. YOSHIDA, M. UEMURA, H. KAWABE and T. YAMADA, in Proceedings of the 13th Japan Congress on Materials Research, 1970, p. 58.
10. V. S. IVANOVA, L. G. ORLOV and V. F. TERENTEV, *Physics of Metals and Metal Science* **33** (1972) 627.
11. V. F. TERENTEV, I. C. KOGAN and L. G. ORLOV, *ibid.* **41** (1976) 601.
12. P. LUKAS, M. KLESNIL and P. RYS, *Z. Metallkde.* **56** (1965) 109.
13. P. LUKAS, M. KLESNIL, in Proceedings of the 2nd Int. Conf. On Corrosion Fatigue, edited by O. J. Devereux, A. J. McEvily, and R. W. Staehl (National Association of Corrosion Engineers NACE, Houston, 1972) p. 118.
14. C. LAIRD, in "Work Hardening in Tension and Fatigue," edited by A. W. Thompson (AIME, New York, 1977) p. 150.
15. J. M. FINNEY and C. LAIRD, *Phil. Mag.* **31** (1975) 339.
16. P. LUKAS, M. KLESNIL and P. RYS, *Phys. Stat. Solidi* **37** (1970) 833.
17. J. D. ASHTON, O. T. WOO and B. RAWASWAMI, *Met. Trans.* 6A (1975) 1957.
18. T. BROOM, J. A. MAZZA and V. N. WHITTAKER, *J. Inst. Met.* 86 (1977) 17
19. A. S. KEH, W. C. LESLIE and D. L. SPONSELLER, in "Precipitation from Iron-Base Alloys," edited by G. R. Speich and J. B. Clark (Gordon and Breach, New York, 1965) p. 281.
20. L. HABRAKEN and T. GREDAY, "Copper in Low Carbon and Low Alloy Steels" (National Centre of Metallurgical Research, Liege, 1965).

Received 16 January
and accepted 3 August 2001